FLT1 Genetic Variation Predisposes to Neovascular AMD in Ethnically Diverse Populations and Alters Systemic FLT1 Expression

Leah A. Owen,[1] Margaux A. Morrison,[1] Jeeyun Ahn,[2] Se Joon Woo,[3] Hajime Sato,[4] Rosann Robinson,[1] Denise J. Morgan,[1] Fani Zacharaki,[5] Marina Simeonova,[6] Hironori Uehara,[1] Usha Chakravarthy,[7] Ruth E. Hogg,[7] Balamurali K. Ambati,[1] Maria Kotoula,[5] Wolfgang Baehr,[1] Neena B. Haider,[8] Giuliana Silvestri,[7] Joan W. Miller,[6] Evangelia E. Tsironi,[5] Lindsay A. Farrer,[9] Ivana K. Kim,[6] Kyu Hyung Park,[2] and Margaret M. DeAngelis[1]

[1]Department of Ophthalmology and Visual Sciences, University of Utah, Salt Lake City, Utah, United States
[2]Department of Ophthalmology, Seoul Metropolitan Government Seoul National University Boramae Medical Center, Seoul, Republic of Korea
[3]Department of Ophthalmology, Seoul National University Bundang Hospital, Seoungnam, Republic of Korea
[4]Department of Ophthalmology, Tohoku University Graduate School of Medicine, Aoba-ku, Sendai, Japan
[5]Department of Ophthalmology, University of Thessaly, School of Medicine, Larissa, Greece
[6]Retina Service, Massachusetts Eye and Ear, Department of Ophthalmology, Harvard Medical School, Boston, Massachusetts, United States
[7]Centre for Experimental Medicine, Queen's University, Belfast, United Kingdom
[8]Schepens Eye Research Institute, Harvard Medical School, Boston, Massachusetts, United States
[9]Departments of Medicine (Biomedical Genetics), Ophthalmology, Neurology, Epidemiology, and Biostatistics, Boston University Schools of Medicine and Public Health, Boston, Massachusetts, United States

Correspondence: Margaret M. DeAngelis, The University of Utah, John A. Moran Eye Center, 65 Mario Capecchi Drive, Salt Lake City, UT 84132, USA;
Margaret.deangelis@utah.edu.

IKK, KHP, and MMD contributed equally to the work presented here and therefore should be regarded as equivalent authors.

Submitted: January 27, 2014
Accepted: April 23, 2014

Citation: Owen LA, Morrison MA, Ahn J, et al. *FLT1* genetic variation predisposes to neovascular AMD in ethnically diverse populations and alters systemic FLT1 expression. *Invest Ophthalmol Vis Sci*. 2014;55:3543–3554. DOI:10.1167/iovs.14-14047

Purpose. Current understanding of the genetic risk factors for age-related macular degeneration (AMD) is not sufficiently predictive of the clinical course. The VEGF pathway is a key therapeutic target for treatment of neovascular AMD; however, risk attributable to genetic variation within pathway genes is unclear. We sought to identify single nucleotide polymorphisms (SNPs) associated with AMD within the VEGF pathway.

Methods. Using a tagSNP, direct sequencing and meta-analysis approach within four ethnically diverse cohorts, we identified genetic risk present in *FLT1*, though not within other VEGF pathway genes *KDR*, *VEGFA*, or *VASH1*. We used ChIP and ELISA in functional analysis.

Results. The *FLT1* SNPs rs9943922, rs9508034, rs2281827, rs7324510, and rs9513115 were significantly associated with increased risk of neovascular AMD. Each association was more significant after meta-analysis than in any one of the four cohorts. All associations were novel, within noncoding regions of *FLT1* that do not tag for coding variants in linkage disequilibrium. Analysis of soluble FLT1 demonstrated higher expression in unaffected individuals homozygous for the *FLT1* risk alleles rs9943922 ($P = 0.0086$) and rs7324510 ($P = 0.0057$). In silico analysis suggests that these variants change predicted splice sites and RNA secondary structure, and have been identified in other neovascular pathologies. These data were supported further by murine chromatin immunoprecipitation demonstrating that *FLT1* is a target of *Nr2e3*, a nuclear receptor gene implicated in regulating an AMD pathway.

Conclusions. Although exact variant functions are not known, these data demonstrate relevancy across ethnically diverse genetic backgrounds within our study and, therefore, hold potential for global efficacy.

Keywords: age-related macular degeneration, angiogenesis, FLT1, VEGF

Age-related macular degeneration (AMD) is a debilitating condition resulting in eventual loss of central vision, which is implicit in functions such as reading, driving, and facial recognition. Currently, AMD represents the leading cause of blindness within the US elderly population.[1] The neovascular form of AMD, characterized by aberrant blood vessel growth beneath the retina, leads to more rapid visual loss. Therefore, it is recognized as a more severe form of the disease and accounts for approximately 85% to 90% of overall legal blindness attributable to AMD.[2] The genetic etiologic factors that predispose an individual to this form of AMD are not fully elucidated. It is clear that family history is an important predictive factor, though AMD is thought to be a multifactorial disease and, thus, not inherited in a Mendelian fashion, and one

that may be influenced by a number of pathways.[3] Certainly, a greater understanding of the underlying molecular and genetic risk factors would aid in our ability to identify early individuals who will have aggressive disease and secondly allow for more targeted therapies to address this pathology.

The central pathophysiology of neovascular AMD, aberrant blood vessel growth clinically termed choroidal neovascularization (CNV), requires alteration of the local balance between angiogenesis stimulators and inhibitors, such that the formation of new vessels is favored. The predominant signaling pathway responsible for physiologic and pathologic ocular angiogenesis is the VEGF pathway. VEGF signaling mediates effect via a family of ligands that bind one or both of two tyrosine kinase receptors, the *FLT1* and *KDR* genes (VEGFR1 and VEGFR2, respectively, in mice).[4] The *KDR* gene has strong tyrosine kinase activity, and is thought to be the primary mediator of angiogenesis.[5,6] The *FLT1* gene has very little kinase activity, but has a complex role during angiogenesis. Murine studies demonstrate that it primarily acts as a "VEGF trap" and, thus, a negative regulator of angiogenesis in the embryo.[7] In adult angiogenesis, *FLT1* has a dual role whereby it has proangiogenic tyrosine kinase activity, though retains its suppressive function via a physiologic splice variant, termed soluble FLT1 (sFLT1).[6] Soluble FLT1 contains only the ligand binding domain and, therefore, functions as an endogenous VEGF inhibitor.[8–10] In addition to sFLT1, Vasohibin 1 (VASH1) is emerging as an important negative regulator of vessel growth. VASH1 is a secretory protein that is produced in a VEGF-dependent manner by vascular endothelial cells.[11] It has been shown to inhibit VEGF-mediated angiogenesis in vitro and in vivo via inhibition of migration and proliferation of endothelial cells.[12] These data are substantiated functionally in VASH1 knock-out mice, which demonstrate aberrant, vascularization extending beyond physiologic boarders.[13]

Increased VEGF expression has been shown in the RPE and in the outer nuclear layer of the macula in early stages of AMD, before the onset of overt neovascularization as well once neovascularization has occurred.[14] Furthermore, overexpression of VEGF in the RPE of rats and mice leads to the development of CNV, and alternatively increased sFLT1 has been shown to decrease the formation of experimental CNV.[8,15,16] At present, to our knowledge there are no studies demonstrating a role for VASH1 in AMD predisposition or pathogenesis. However, laser-induced models of CNV in mice have shown that VASH1 is upregulated within the retina following laser insult, and that its expression correlates temporally with regression of the CNV lesions.[17] Furthermore, increased intraocular expression of VASH1 suppressed retinal neovascularization in monkey and rat models of ischemic retinopathy.[11,18] Thus, these angiogenesis mediators are relevant to the disease pathogenesis of AMD and, therefore, they may represent novel genetic predictors of disease.

Current therapies for neovascular AMD target established aberrant blood vessel growth through antibody-based inhibition of VEGF and demonstrate a range of efficacy.[19–21] Indeed, for a subset of patients, these therapies result in stable to improved visual acuity without the need for ongoing treatment.[20,21] However, the majority of patients require indefinite treatment or demonstrate progression of disease despite treatment.[20–22] Therefore, a better understanding of the predisposing genetic factors important for development of AMD and genetic biomarkers useful in the identification of those at risk is vital to identifying individuals likely to develop neovascular disease and perhaps predicting their response to therapy. Continued study of genetic variation in AMD may also lead to disease prevention.

At present, variants within *CFH* and *HTRA1/ARMS2* genes appear to be the genetic risk factors associated most strongly with AMD.[23–26] However, variation at these 2 loci is not strongly predictive of specific phenotypic manifestations of AMD. Therefore, our current understanding of the predisposing genetic risk factors is insufficient. Furthermore, these polymorphisms are not associated significantly with the final common pathology of aberrant blood vessel growth.

Due to the specific nature of the pathology in neovascular AMD, assessment of VEGF pathway variants that correlate with the neovascular disease state may allow for greater understanding of genetic risk factors and overall pathophysiology. Several polymorphisms within and around *VEGFA* have been associated with AMD, a number of which have been postulated to be disease modifiers,[27–32] including the largest genome-wide association study (GWAS) to date by the AMD Gene Consortium, which found two single nucleotide polymorphisms (SNPs) within linkage disequilibrium (LD).[24] Additionally, preliminary work within the northern Indian subcontinent population demonstrates an SNP within *KDR* (rs1531289) that is associated significantly with AMD showing disproportionate levels within neovascular AMD.[33] Although an association between *FLT1* SNPs and response to AMD treatment is described,[19] to our knowledge there have been no studies showing association between *FLT1* SNPs and risk of AMD. Despite these findings, other studies have failed to find an association with VEGF pathway polymorphisms, including, *FLT1,* and neovascular AMD.[31,34]

The role of genetic variation within the VEGF pathway and AMD risk remains an unresolved and important question with treatment implications going forward. We hypothesized that genetic risk of neovascular AMD is present within the VEGF pathway as it is fundamental to the balance between pro- and antiangiogenesis signaling.

Methods

Family-Based Patient Cohort

The protocol was reviewed and approved by the Institutional Review Boards at the Massachusetts Eye & Ear Infirmary (MEEI; Boston, MA, USA), and the University of Utah (Salt Lake City, UT, USA), and conforms to the tenets of the Declaration of Helsinki. Eligible patients were enrolled in this study after they gave informed consent either in person, over the phone, or through the mail, before answering questions to a standardized questionnaire and donating 10 to 50 mL of venous blood.

Details of the recruitment of the sibling pairs (the New England Sibpair Cohort; NESC), comprised mainly of individuals of European ancestry, have been described in detail previously.[35,36] Briefly, disease status of every participant was confirmed by at least two investigators by evaluation of fundus photographs or fluorescein angiograms, except when one of the investigators directly examined an unaffected sibling during a home visit ($n = 4$ cases).

All index patients were 50 years of age or older and had the neovascular form of AMD in at least one eye, defined by subretinal hemorrhage, fibrosis, or fluorescein angiographic presence of neovascularization. Patients whose only neovascular finding was a RPE detachment were excluded, because this finding may not represent definite neovascular AMD. Patients with signs of pathologic myopia, presumed ocular histoplasmosis syndrome, angioid streaks, choroidal rupture, any hereditary retinal diseases other than AMD, and previous laser treatment due to retinal conditions other than AMD, also were excluded.

Table 1. Patient Characteristics in the Discovery (NESC) and Cohort Patient Groups (BSC, Greek, and Korean)

	Controls	Dry AMD	Geographic Atrophy	Neovascular AMD
NESC				
Total *n*	198	106	12	341
Average age (range)	75.4 (50.3–94.3)	77.6 (58.2–100.6)	78.9 (58.4–94.0)	73.7 (49.0–92.0)
Males (% total)	87 (0.44)	37 (0.35)	5 (0.42)	139 (0.41)
BSC				
Total *n*	52	0	5	62
Average age (range)	70.0 (50.0–87.1)	n/a	77.0 (62.0–95.1)	79.0 (56.0–96.1)
Males (% total)	21 (0.40)	n/a	2 (0.4)	20 (0.32)
Greek				
Total *n*	213	68	16	139
Average age (range)	73.8 (48.0–95.0)	74.4 (53.0–91.0)	76.1 (56.0–85.0)	76.3 (49.0–94.0)
Males (% total)	100 (0.47)	28 (0.41)	10 (0.625)	63 (0.45)
Korean				
Total *n*	682	163	46	321
Average age (range)	72.1 (48.0–99.0)	71.9 (55.0–88.0)	72.8 (58.0–90.0)	71.7 (43.0–92.0)
Males (% total)	332 (0.49)	51 (0.31)	21 (0.46)	177 (0.55)

Patients with an early/intermediate form of AMD were classified according to the Age-Related Eye Disease Study (AREDS) as either category 2 (small [<63 μm] drusen with total area ≥ 125 μm diameter circle, or at least 1 intermediate druse [≥63 and <125 μm], or presence of pigment abnormalities), or AREDS category 3 (intermediate drusen comprising a total area ≥ 360 μm diameter circle in the presence of soft drusen, or a ≥656 μm diameter circle in absence of soft drusen, or at least 1 large druse [≥125 μm], or noncentral geographic atrophy), as previously described for this cohort.[37]

The unaffected siblings had normal maculae and were at least 65 years or older at the time at which the index patient was first diagnosed with neovascular AMD. These criteria are based on published epidemiologic studies that indicate that elderly individuals with such maculae rarely go on to have neovascular AMD during a 10-year follow-up. Unaffected maculae fulfilled the following criteria: 0 to 5 small drusen (all less than 63 μ in diameter), no pigment abnormalities, no geographic atrophy, and no neovascularization (as defined previously; AMD "category 1 or less" on the AREDS scale).[3]

Replication Cohorts

Replication of significant findings was performed on an additional family-based cohort and two unrelated case-control cohorts. The second family-based cohort, the Belfast Sibpair Cohort (BSC), was recruited from Northern Ireland and details have been described previously.[38] The central Greece cohort (Greek), as described previously,[39] includes patients recruited from Larissa, Greece. The Korean cohort (Korean) was recruited from the Seoul National University Bundang Hospital (SNUBH; Seoul, Kores) retina clinic from July 2008 to October 2010 and has yet to be described in detail.[24] Briefly, all patients underwent comprehensive ophthalmologic evaluation, including measurement of best-corrected visual acuity, slit-lamp biomicroscopy, indirect fundus exam, fluorescein angiography (FA), indocyanine green angiography (ICGA, Heidelberg Retina Angiography; Heidelberg Engineering, Heidelberg, Germany), and optical coherence tomography (OCT, Spectralis OCT; Heidelberg Engineering). Other retinal or choroidal diseases, including pathologic myopia, angioid streaks, presumed ocular histoplasmosis, or secondary CNVs, were excluded. Subjects without any sign of AMD were enrolled as control. They had no drusen or pigment abnormalities in the fundus photograph and/or OCT. Table 1 shows descriptive statistics for each cohort.

SNP Selection

Initially, in a smaller subset of the NESC ($n = 135$ sib pairs discordant for neovascular AMD), a tag SNP (TagSNP) approach was used that encompassed the entire genomic sequence of each gene, including at least −1000 base pairs (bps) upstream region from the transcription start site and +600 base pairs to encompass the 3′-untranslated region. The TagSNPs were selected using the tagger pairwise method, with $r^2 > 0.8$ and minor allele frequency > 0.05 to capture variation within each gene. This was based on the CEU population from the publicly available HapMap data (Rel 23a on NCBI B36, available in the public domain at http://hapmap.ncbi.nlm.nih.gov/downloads/index.html.en accessed November 6, 2008). Briefly, TagSNPs were chosen to cover the 193,442 bp of the *FLT1* gene (Ensembl gene accession number; ENSG00000102755), the 20,823 bp of the *VASH1* gene (ENSG00000071246), the 16,279 bp of the *VEGFA* gene (ENSG00000112715), and the 47,104 bp of the *KDR* gene (ENSG00000128052). In addition to the TagSNPs, further SNPs were chosen due to their previous association with AMD or other related diseases. The SNPs rs13207351, rs1570360, rs2010963, rs1413711, rs833070, rs735286, rs3025020, rs3025021, and rs3025039 in the *VEGFA* gene were chosen for their previous association with AMD.[40] The SNP rs1870377 in *KDR* gene was for previous association with coronary heart disease.[41] The SNP C519T in the *FLT1* gene was chosen for its association with FLT1 expression.[42]

After analyzing the first group of SNPs, additional TagSNPs were chosen based on the following criteria: surrounded SNPs that were initially significant ($P < 0.05$), had a minor allele frequency of at least 10%, and also tagged for at least 6 other SNPs. The additional SNPs tested that fit these criteria were rs622227, rs7324510, rs9943922, and rs10871266 in the *FLT1* gene. Additionally, direct sequencing was performed on exons 4, 5, 9, 10, and 11, as well as at least 100 bps surrounding exonic/intronic boundaries due to significance found in that region in the initial screening of TagSNPs. Direct sequencing also was performed on the promoter and exon 1 of *VASH1* and *VEGFA*.

Genotyping Analysis

Genotyping was performed on leukocyte DNA that was purified by using standard phenol–chloroform or DNAzol (Invitrogen, Carlsbad, CA, USA) extraction protocols.

Multiplex PCR assays were designed using Sequenom SpectroDESIGNER software (version 3.0.0.3; Sequenom, San Diego, CA, USA) by inputting sequence containing the SNP site and 100 bp of flanking sequence on either side of the SNP. Briefly, 10 ng of genomic DNA was amplified in a 5 uL reaction containing ×1 HotStar Taq PCR buffer (Qiagen, Valencia, CA, USA), 1.625 mM MgCl2, 500 uM each dNTP, 100 nM each PCR primer, and 0.5 U HotStar Taq (Qiagen). The reaction was incubated at 94°C for 15 minutes followed by 45 cycles of 94°C for 20 seconds, 56°C for 30 seconds, 72°C for 1 minute, followed by 3 minutes at 72°C. Excess dNTPs then were removed from the reaction by incubation with 0.3 U shrimp alkaline phosphatase (USB Corporation, Cleveland, OH, USA) at 37°C for 40 minutes followed by 5 minutes at 85°C to deactivate the enzyme. Single primer extension over the SNP was carried out in a final concentration of between 0.625 uM and 1.5 uM for each extension primer (depending on the mass of the probe), iPLEX termination mix (Sequenom), and 1.35 U iPLEX enzyme (Sequenom), and cycled using a two-step 200 short cycles program; 94°C for 30 seconds followed by 40 cycles of 94°C for 5 seconds, 5 cycles of 52°C for 5 seconds, and 80°C for 5 seconds, then 72°C for 3 minutes. The reaction then was desalted by addition of 6 mg cation exchange resin followed by mixing and centrifugation to settle the contents of the tube. The extension product then was spotted onto a 384-well SpectroCHIP (Sequenom) before being flown in the MALDI-TOF mass spectrometer. Data were collected, real time, using SpectroTYPER Analyzer 3.3.0.15, SpectraAQUIRE 3.3.1.1, and SpectroCALLER 3.3.0.14 (Sequenom). Additionally, to ensure data quality, genotypes for each subject also were checked manually.

For direct sequencing, oligonucleotide primers were selected using the Primer3 program (available in the public domain at http://primer3.sourceforge.net/) to encompass the exon and flanking sequences. All PCR assays were performed using genomic DNA fragments from 20 ng of leukocyte DNA in a solution of ×10 PCR buffer containing 25 mM of $MgCl_2$, 0.2 mM each of dATP, dTTP, dGTP, and dCTP, and 0.5 units of Taq DNA polymerase (USB Corporation). Then, 5 M Betaine was added to the reaction mix for rs2414687 (Sigma-Aldrich, St. Louis, MO, USA). The temperatures used during the polymerase chain reaction were as follows: 95°C for 5 minutes followed by 35 cycles of 58°C for 30 seconds, 72°C for 30 seconds, and 95°C for 30 seconds, with a final annealing at 58°C for 1.5 minutes and extension of 72°C for 5 minutes. For sequencing reactions, PCR products were digested according to manufacturer's protocol with ExoSAP-IT (USB Corporation) then were subjected to a cycle sequencing reaction using the Big Dye Terminator v3.1 Cycle Sequencing kit (Applied Biosystems, Foster City, CA, USA) according to manufacturer's protocol. Products were purified with Performa DTR Ultra 96-well plates (Edge Biosystems, Gaithersburg, MD, USA) to remove excess dye terminators. NextGen sequencing was performed on exonic regions using methods that have been described previously.[43] For direct sequencing, samples were sequenced on an ABI Prism 3100 DNA sequencer (Applied Biosystems). Electropherograms generated from the ABI Prism 3100 were analyzed using the Lasergene DNA and protein analysis software (DNASTAR, Inc., Madison, WI, USA). Electropherograms were read by two independent evaluators without knowledge of the subject's disease status. All patients were sequenced in the forward direction (5′ to 3′), unless variants or polymorphisms were identified, in which case confirmation was obtained in some cases by sequencing in the reverse direction.

sFLT1 Analysis

Serum samples were collected, aliquoted, and frozen at −80. The levels of sFLT1 were determined on a subset of samples from the discovery cohort ($n = 322$) quantitatively with a Quantikine ELISA kit (sVEGFR1/Flt-1, catalog #SVR100B; R&D Systems, Minneapolis, MN, USA). The samples were assayed following the manufacturer's protocol exactly, using 100 µl of serum per well. Plates were read on a BioTek Synergy 4 (BioTek, Winooski, VT, USA) plate reader at 450 nm with wavelength correction. The corrected optical density readings for samples, controls, and standards, were imported into Prism GraphPad (GraphPad Software, Inc., La Jolla, CA, USA), which interpolated optical densities for all unknowns based on the standard curve.

Statistical Analyses

Deviation from Hardy-Weinberg Equilibrium (HWE) was tested for each SNP using the χ^2 test in unaffected subjects only. The SNPs were tested for association using the minor allele, as defined by the allele occurring less frequently in the unaffected subjects, for all cohorts examined. Initial testing of association between the variation and neovascular AMD in a subset of 135 sibling pairs from the NESC (discovery cohort) was performed using Family Based Association Tests (FBAT). For validation in the sibling cohorts, allelic associations were performed using conditional logistic regression (CLR) in SAS (v9.2; SAS Institute, Inc., Cary, NC, USA). For replication in the unrelated case control cohorts, allelic associations were performed using logistic regression in SAS. Separate association tests were performed for dry AMD, neovascular AMD, and all AMD subtypes together. All haplotypic associations were performed using the program UNPHASED (available in the public domain at http://www.mrc-bsu.cam.ac.uk/personal/frank/software/unphased/). For the family data, the model for sibships was used. UNPHASED uses likelihood ratio association analysis, and sibships uses nuclear families with missing parental genotype data.[44] For the most significant SNPs, haplotype analysis was performed with a sliding window approach.

Additionally, to test for the effects of the VEGF pathway as a whole, a binning approach was used similar to the Data Adaptive Sum (DAS) method.[45] The most significant SNP from each gene in the pathway was selected and combined with the SNPs from the other genes to create a binned pathway variable, which was tested for its association with AMD.

Haploview (available in the public domain at http://www.broad.mit.edu/mpg/haploview/) was used to generate the linkage disequilibrium plots for each of the genes tested.

Replication of significant findings was performed in 3 additional separate cohorts. Meta-analysis was performed for SNPs genotyped in all four cohorts using the program Comprehensive Meta-Analysis v2 (Biostat, Englewood, NJ, USA). Z scores and overall P values for each SNP were calculated under a fixed model based on individual odds ratios (ORs) and confidence intervals (CIs) for each cohort, as calculated in SAS. To test for the effects of population heterogeneity, Cochran's Q also was calculated, which is the weighted sum of squared differences between individual study effects and the pooled effect across studies. Factors showing significant heterogeneity were evaluated under a random effects model.

Serum soluble FLT1 outliers were considered outside 3 SDs from the mean and, thus, were remeasured to confirm. The confirmed measurements were analyzed as a continuous

variable and tested for association with AMD in the sibpairs using CLR. Unadjusted and analyses adjusted for age and sex were performed. Additionally, sFLT1 was tested for interaction with the significant SNPs by adding an interaction term into the CLR model.

In Silico Splice Site Analysis

The *FLT1* mRNA sequence was obtained via ENSEMBL Build36 accessed on 4.1.13. The *FLT1* RNA sequence with either the common or minor (SNP) allele for each of the five significant *FLT1* SNPs was assessed. Analysis was performed using the Berkeley Drosophila Genome Project splice site prediction software (available in the public domain at http://www.fruitfly.org/) with a minimum score of 0.4 for the 5′ and 3′ splice sites for all five significant SNPs; data reported for rs7324510 were generated using a minimum score of 0.4 for the 5′ and 3′ splice sites; however, as splicing changes were initially not noted with a score of 0.4. A second analysis was performed on the same sequence data using Alternative Splice Site Predictor (ASSP, available in the public domain at http://wangcomputing.com/assp/index.html) using a false splice site cutoff for acceptor sites of 2.2 and false splice site cutoff for donor sites of 4.5.[46]

RNA Secondary Structure Analysis

The *FLT1* mRNA sequence was obtained via ENSEMBL Build36 accessed on 4.1.13. One KB of *FLT1* RNA sequence flanking either the common or the minor (SNP) allele for each of the five significant *FLT1* SNPs was assessed. Analysis was performed using CentroidFold (available in the public domain at http://www.ncrna.org/centroidfold).

Methylation Analysis

The *FLT1* mRNA sequence was obtained via ENSEMBL Build36 accessed on 4.1.13. Assessment of peak methylation sites was performed using the Human Histone Modification Database (available in the public domain at http://202.97.205.78/hhmd/index.jsp). The bp locations demonstrating peak methylation were compared to SNP location to assess for alterations.

Animal Maintenance

Animals were housed in vivariums at the Schepens Eye Research Institute and the Nebraska Medical Center; use and procedures were approved by the Animal Care and Use Committee and conducted in compliance with the Animal Welfare Act Regulations and the ARVO Statement for the Use of Animals in Ophthalmic and Vision Research. Mice were housed in microisolator cages, and provided food and water ad libitum. The University of Nebraska Medical Center and Schepens Eye Research Institute are in compliance with the National Institutes of Health (NIH) policy on the use of animals in research (Animal Welfare Act P.L. 89–544, as amended by P.L. 91–579 and P.L. 94–279) as well as the Guide for the Care and Use of Laboratory Animals, NIH Publication No. 86–23. Tissues were harvested from $Nr2e^{3rd7/rd7}$ and C57BL6/J mice at postnatal day 30 (P30). A minimum of three animals were analyzed.

Chromatin Immunoprecipitation

Chromatin immunoprecipitation was performed as described previously.[47] The *FLT1* response element (RE) binding site was identified using a classic binding motif of Nr2e3 (AAGTCA[n1–4]AAGTCA) and a general nuclear hormone receptor response elements as determined algorithmically by NUBIscan (M. Podvinec and University of Basel, Basel, Switzerland). The RE sites were evaluated at a maximum of 30 kb upstream of each gene's start site to intron 1.

Quantitative Real-Time PCR

Quantitative RT-PCR was performed using 1 μl of 1:100 dilution (input) and 1:10 dilution (samples and IgG control) using conditions described previously.[47,48] All sample data were normalized to Ig control. Briefly, retinas were dissected rapidly after eye enucleation and placed in Trizol (Invitrogen) for RNA extraction. Eyes were collected consistently in the early afternoon for each animal to eliminate variability due to circadian expression. Total RNA (2 μg) was reverse transcribed using Retroscript (Ambion, Austin, TX, USA). Real-time PCR was performed in technical triplicates with a minimum of three biological replicates using SYBR Green PCR master mix (Applied Biosystems). Reactions were quantified using a Roche 480 LightCycler (Roche Applied Sciences, Indianapolis, IN, USA) real-time PCR instrument. Relative expression levels were normalized to the amount of β-actin expressed and fold change relative to wild-type C57BL/6J control was calculated using the delta Ct method. Standard error was calculated to determine statistical significance.

Results

Identification of SNPs Significantly Associated With the Neovascular AMD Phenotype

Tag SNPs were identified using the HapMap for the VEGF pathway genes *KDR*, *VEGFA*, *VASH1*, and *FLT1*. Using these tag SNPs within the discovery subset of the NESC cohort ($n = 135$ sibpairs discordant for neovascular AMD), variation was observed within 99 SNPS within these four genes, including deletions and insertions in the VEGF-signaling pathway (see Supplementary Table S1). No SNPs showed deviation from HWE. Initial single SNP analysis showed modest associations between neovascular AMD and one SNP in *KDR*, four SNPs in *VEGFA*, and one SNP in *VASH1*, but these results did not remain significant after correcting for multiple testing. After correcting for multiple testing, single SNP analysis showed significant associations between five *FLT1* SNPs and neovascular AMD. The most significant association was seen in rs9508034, which was shown to increase risk of neovascular AMD 2.3-fold ($P = 0.0078$) under a dominant genetic model. Replication of the *FLT1* SNPs in the remainder of the NESC, including all AMD subtypes, included 12 SNPs; those that were significant in the original analysis (either significant individually or as part of a significant haplotype defined by the Gabriel rule: rs638889, rs732184, rs9513115, rs9513113, rs9554330, rs2281827, rs9508034, and rs11149523) and the second set of TagSNPs chosen to determine the contribution of further variation in this region (rs1087266, rs9943922, rs7324510, and rs622227). From this replication, 7 SNPs remained significantly associated with neovascular AMD and, thus, were genotyped in the remaining replication cohorts: *VASH1* rs2270324, *VEGFA* rs2010963, and *FLT1* SNPs rs9943922, rs9508034, rs2281827, rs7324510, and rs9513115. The resulting genotyping and analysis showed that five *FLT1* SNPs remained significantly associated with neovascular AMD in the NESC and/or Greek cohorts, while the *VEGFA* and *VASH1* SNPs did not (Table 2). Specifically, the minor alleles of the *FLT1* SNPs rs9943922, rs9508034, rs2281827, rs7324510, and rs9513115 were all significantly associated with increased risk of all AMD subtypes

Table 2. Meta-analysis of Single SNP Analysis for Each Cohort, Comparing Neovascular Cases to Normal Subjects

		Additive		Dominant		Recessive	
Comparison	**Study**	**OR (95% CI)**	***P* Value**	**OR (95% CI)**	***P* Value**	**OR (95% C.I.)**	***P* Value**
Vash1 rs2270324	Greek	1.067 (0.670–1.699)	0.7846	1.039 (0.615–1.755)	0.8863	1.522 (0.303–7.650)	0.6102
	BSC	0.899 (0.338–2.391)	0.8312	0.771 (0.264–2.247)	0.6334	n/a	n/a
	Korean	0.954 (0.731–1.246)	0.7292	0.918 (0.676–1.247)	0.5844	1.194 (0.521–2.735)	0.6750
	NESC	1.248 (0.759–2.055)	0.3827	1.439 (0.821–2.520)	0.2034	0.404 (0.067–2.439)	0.3230
Meta		1.018 (0.829–1.250)	0.8658	1.009 (0.799–1.274)	0.9419	1.067 (0.539–2.110)	0.8527
VEGFA rs2010963	Greek	0.995 (0.724–1.368)	0.9754	0.990 (0.620–1.580)	0.9664	1.001 (0.561–1.785)	0.9973
	BSC	1.012 (0.597–1.717)	0.9648	0.944 (0.425–2.096)	0.8878	1.166 (0.397–3.429)	0.7800
	Korean	1.062 (0.872–1.293)	0.5487	1.148 (0.856–1.540)	0.3569	0.991 (0.688–1.428)	0.9613
	NESC	1.039 (0.801–1.349)	0.7710	1.068 (0.744–1.535)	0.7207	1.019 (0.599–1.734)	0.9444
Meta		1.040 (0.908–1.192)	0.5721	1.081 (0.886–1.318)	0.4438	1.009 (0.779–1.308)	0.9457
FLT1 rs2281827	Greek	1.418 (0.969–2.076)	0.0724	1.595 (1.015–2.506)	0.0428	1.132 (0.393–3.261)	0.8184
	BSC	1.009 (0.502–2.030)	0.9792	1.453 (0.635–3.323)	0.3759	n/a	n/a
	Korean	1.023 (0.832–1.258)	0.8293	1.214 (0.925–1.593)	0.1620	0.615 (0.370–1.021)	0.0602
	NESC	1.458 (1.060–2.004)	0.0203	1.694 (1.163–2.468)	0.0060	1.042 (0.451–2.405)	0.9237
Meta		1.171 (1.004–1.366)	0.0440	1.406 (1.160–1.704)	0.0005	0.758 (0.507–1.132)	0.1757
FLT1 rs9513115	Greek	1.501 (1.030–2.187)	0.0344	1.564 (0.989–2.474)	0.0559	2.035 (0.763–5.426)	0.1556
	BSC	1.391 (0.699–2.769)	0.3473	1.849 (0.757–4.514)	0.1773	0.811 (0.156–4.225)	0.8039
	Korean	1.093 (0.887–1.346)	0.4032	1.238 (0.941–1.629)	0.1273	0.831 (0.513–1.346)	0.4519
	NESC	1.207 (0.889–1.637)	0.2278	1.235 (0.860–1.775)	0.2537	1.351 (0.576–3.169)	0.4885
Meta		1.195 (1.025–1.392)	0.0225	1.314 (1.083–1.593)	0.0055	1.040 (0.715–1.515)	0.8362
FLT1 rs9943922	Greek	1.509 (1.118–2.037)	0.0072	1.896 (1.113–3.229)	0.0185	1.650 (1.035–2.629)	0.0351
	BSC	0.860 (0.482–1.535)	0.6100	1.296 (0.475–3.540)	0.6127	0.577 (0.238–1.401)	0.2242
	Korean	1.051 (0.868–1.272)	0.6096	1.287 (0.930–1.781)	0.1280	0.899 (0.657–1.231)	0.5062
	NESC	1.154 (0.893–1.492)	0.2743	1.347 (0.892–2.034)	0.1569	1.082 (0.711–1.645)	0.7140
Meta		1.145 (1.002–1.307)	0.0463	1.398 (1.117–1.749)	0.0034	1.046 (0.844–1.296)	0.6822
FLT1 rs7324510	Greek	1.338 (0.930–1.925)	0.1167	1.333 (0.855–2.079)	0.2048	1.970 (0.757–5.126)	0.1647
	BSC	1.333 (0.647–2.745)	0.4361	1.543 (0.649–3.668)	0.3265	0.902 (0.122–6.665)	0.9194
	KOREAN	1.048 (0.848–1.295)	0.6642	1.188 (0.904–1.562)	0.2169	0.731 (0.437–1.223)	0.2327
	NESC	1.188 (0.865–1.632)	0.2873	1.190 (0.824–1.718)	0.3547	1.471 (0.561–3.858)	0.4327
Meta		1.141 (0.977–1.332)	0.0947	1.230 (1.015–1.490)	0.0345	0.992 (0.663–1.482)	0.9669
FLT1 rs9508034	GREEK	1.467 (1.018–2.114)	0.0398	1.564 (0.998–2.451)	0.0510	1.735 (0.701–4.294)	0.2334
	BSC	0.929 (0.476–1.811)	0.8285	1.400 (0.624–3.141)	0.4150	n/a	n/a
	KOREAN	1.036 (0.836–1.284)	0.7466	1.178 (0.893–1.553)	0.2459	0.703 (0.416–1.188)	0.1880
	NESC	1.505 (1.064–2.130)	0.0210	1.774 (1.176–2.674)	0.0062	1.061 (0.443–2.541)	0.8941
Meta		1.188 (1.014–1.393)	0.0329	1.383 (1.135–1.686)	0.0013	0.917 (0.613–1.372)	0.6748

(data not shown), but most significantly the neovascular AMD phenotype in meta-analysis of the 4 cohorts.

Each of the five significant *FLT1* SNPs was most significantly associated with neovascular AMD under a dominant model, indicating that the effect was not dose-dependent.[49,50] The most significant of these SNPs, rs9943922, was shown to increase risk of neovascular AMD by 1.481-fold ($P = 0.0037$), which was similar for the other significantly associated SNPs. Most importantly, for each *FLT1* SNP, the results of meta-analysis of the four cohorts produced more significant associations than were found in any one cohort alone. Additionally, in each of the four cohorts, the dominant model showed the same direction of effect, increased risk, and there was no evidence of heterogeneity in any of the comparisons or across comparisons, as the *P* value of Cochran's Q was not significant ($P > 0.05$). Results of the binned SNP pathway analysis and haplotype analysis showed that no binned variable or haplotype was more significant than any single SNP (results not shown).

The LD was high between SNPs rs9508034 and rs2281827, and SNPs rs7324510 and rs9513115 in all cohorts, indicating two distinct signals ($r^2 > 0.74$ for all, Supplementary Fig. S1). In the Korean cohort, these SNPs were all in high LD, indicating one signal. Therefore, LD was similar among the Caucasian cohorts, but not with the Korean cohort.

Functional and In Silico Analysis of Significant FLT1 SNPs

To determine if presence of the five significant *FLT1* variants correlated with systemic FLT1 expression, sFLT1 was measured in the serum of patients within the discovery cohort using ELISA. This analysis demonstrated no significant association between sFLT1 levels and AMD (Table 3). Interestingly, there was significant interaction between sFLT1 and *FLT1* SNPs rs9943922 and rs7324510 ($P < 0.01$). Specifically, normal subjects homozygous for the risk alleles at *FLT1* SNPs rs9943922 and rs7324510 had significantly higher sFLT1 (Fig. 1).

To understand the possible functional role for the five significant *FLT1* SNPs, we performed targeted genomic and in silico analysis. Sequencing of the flanking exonic and intronic/exonic boundary genomic DNA for each of the five SNPs demonstrated no functional mutations in linkage disequilibrium. Further analysis of these SNPs revealed no evidence of changes to areas of peak methylation as determined by the Human Histone Modification Database. To determine if presence of the significant *FLT1* SNPs results in a splicing change, constitutive splice sites within 200 bp flanking either the major or minor allele for each of the *FLT1*, SNPs was done using the Berkley Drosophila Genome Project. This analysis

Table 3. Association of Serum sFLT1 and Neovascular AMD in Discovery Cohort ($n = 322$)

Variable	OR	95% CI Low	95% CI High	*P* Value
sFLT1, ng/mL	0.997	0.992	1.002	0.2762
sFLT1, ng/mL, adjusted*	0.994	0.981	1.007	0.3360
VASH1 rs2270324/sFLT1 int.	0.998	0.980	1.016	0.8129
VEGFA rs2010963/sFLT1 int.	0.999	0.978	1.019	0.8962
FLT1 rs2281827/sFLT1 int.	1.004	0.995	1.012	0.4142
FLT1 rs9513115/sFLT1 int.	1.008	0.993	1.023	0.3023
FLT1 rs9943922/sFLT1 int.	0.972	0.952	0.993	0.0086
FLT1 rs7324510/sFLT1 int.	0.970	0.949	0.991	0.0057
FLT1 rs9508034/sFLT1 int.	0.985	0.971	1.000	0.0501

int., interaction.
* Adjustment made for age and sex.

demonstrates a change in predicted acceptor site for SNP rs9508034 located within intron 10. It further demonstrates creation of novel acceptor and donor sites within intron 4 in the presence of the rs7324510 minor allele. Analysis of the same sequence data using the ASSP demonstrated generation of a novel acceptor splice site for SNP rs9508034 when compared to the common allele (TTCATCACAGAGCAGG CACT; minor allele is denoted with underlined nucleotide).[46]

To assess for potential changes in RNA secondary structure, analysis of predicted RNA secondary structure for each of the five *FLT1* SNPs was performed using tools available in the public domain at www.ncRNA.org. Assessment based on 500 bp of RNA sequence flanking either the common or minor allele reveals changes to the predicted RNA secondary structure and required folding energy for all of the significant *FLT1* SNPs. In this analysis, SNPs rs9508034, rs2281827, and rs9513115 showed a decreased energy of folding for the minor allele when compared to the major allele, while rs9943922 and rs7324510 demonstrated an increased energy requirement for proposed minor allele secondary structure. We also assessed for predicted RNA secondary structure of the minor versus major allele SNP sequences based on homologous sequences of the target.[51] In this analysis only SNPs rs9508034 and rs2281827 demonstrated a change in their predicted secondary structures for the minor versus major allele sequences.

Our prior studies and those of others have demonstrated the nuclear hormone receptor Nr2e3 as a key regulator of retinal development and function.[52–55] Further, our recent studies have implicated *Nr2e3* in modulating gene networks related to AMD.[39,56] To identify factors regulating *FLT1* expression, we performed chromatin immunoprecipitation using normal mouse retinas from C57BL/6J animals. We identified a consensus Nr2e3 binding response element (AAGTCANAAGTCA) in the 5′ untranslated region of *FLT1* and determined that Nr2e3 binds to and, therefore, may regulate expression of *FLT1* (Fig. 2).

Discussion

Herein, we described five SNPs within the *FLT1* gene that were more significant in meta-analysis than in any one of the 4 cohorts for risk of neovascular AMD. Additionally, these cohorts, although diverse in ethnicity, showed no statistically significant heterogeneity, as evidenced by a nonsignificant Cochran's Q test. Though initially significant in the discovery cohort, other SNPs identified within VEGF pathway genes, including *KDR*, *VEGFA*, and *VASH1*, did not demonstrate significance in the replication cohorts. Therefore, these data suggest that in the present study genetic variation within the *FLT1* gene, but not *KDR*, *VEGFA*, or *VASH1* genes, may predispose to neovascular AMD. Interestingly, the most significant genetic model was a dominant model indicating that presence of at least one risk allele at each of these variants produces the most risk and that the effect is not dose-dependent. This is similar to what has been found for other complex diseases.[49,50]

Current Understanding of Pathologic FLT1 Function

The current neovascular AMD treatment paradigm is centered largely on VEGFA inhibition, as the VEGF pathway is central to AMD pathophysiology.[19,57] Analysis and therapeutic targeting of VEGF pathway meditators is an evolving area of investigation. FLT1 is a receptor tyrosine kinase that, in concert with its

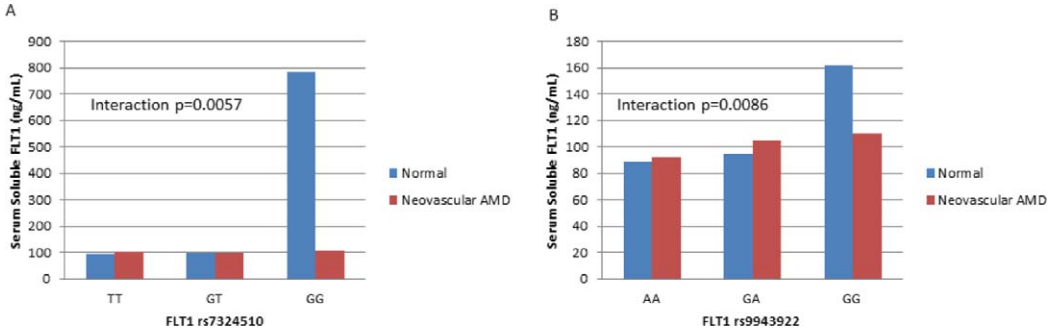

Figure 1. sFLT1 interaction with *FLT1* SNPs and Neovascular AMD. Serum was obtained from the discovery cohort and soluble FLT1 levels were determined using ELISA. Statistical analysis was performed for the interaction between each *FLT1* SNP, sFLT1, and neovascular AMD. The interaction *P* for SNPs rs7324510 (**A**) and rs9943922 (**B**) demonstrate significance between these three variables. In patients with these SNPs, serum sFLT1 were elevated in patients with two risk alleles.

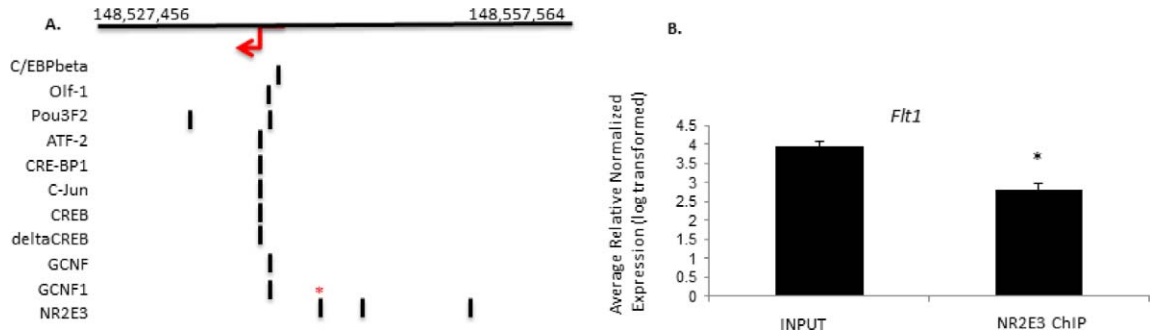

Figure 2. Nr2e3 binds *Flt1* regulatory sequence. (**A**) Transcription factor binding sites for murine *Flt1*. Region represent nucleotides 148,527,456 to 148,557,564 on mouse chromosome 5. Red arrow indicates *Flt1* transcriptional start site. Bars indicate approximate location of binding sites. *Red asterisk* indicates Nr2e3 RE site identified by Chromatin immunoprecipitation (ChIP). (**B**) ChIP-qPCR showing the nuclear hormone receptor Nr2e3 binds *Flt1* regulatory sequence.

counterpart KDR, mediates the process of angiogenesis within this pathway.[58,59] Functionally, FLT1 has been shown to modulate new vessel growth from existing vasculature, maintain endothelial cells, and promote vascular permeability in response to several ligands within the VEGF family.[60] Despite the fact that FLT1 and KDR share high sequence homology and bind many of the same ligands, it long has been believed that KDR is the primary receptor by which VEGF mediates angiogenesis.[61] Thus, FLT1 is viewed as less potent with regard to physiologic as well as pathologic angiogenesis and vascular permeability, and as such, is not classically felt to be a viable therapeutic target.

Accumulating evidence, however, suggests that FLT1 signaling has an important role in pathologic angiogenesis, mediated by not only VEGFA, but also placental growth factor (PlGF), a specific ligand for FLT1.[62–64] Recent work done in a laser-induced murine model of CNV as well as oxygen fluctuation mediated ischemic retinopathy and retinal neovascularization, demonstrated that antibody blockade of FLT1 resulted in suppression of choroidal and retinal neovascularization in a dose-dependent manner.[65] Interestingly, these findings were true for FLT1 as well as KDR inhibition individually. Furthermore, the efficacy was enhanced when the antibodies were used in combination, providing evidence that both receptors have a role in aberrant neovascularization.[65] In these same models of retinal neovascularization, antibody blockade of PIGF demonstrated similar findings.[66,67] These data were substantiated in work using a laser photocoagulation model of CNV in the murine retina, which demonstrated a dose-dependent regression of established CNV following intraocular injection with anti-PIGF antibody.[68] Also, gene therapy with sFLT1 has been shown to be effective in a primate model of laser-induced CNV.[6] Thus, there is substantial backing for a role for FLT1 in pathogenesis and treatment of neovascular AMD.

Potential Significance of *FLT1* SNPs

The functional significance of these novel AMD-associated *FLT1* SNPs is unclear, as they fall within noncoding regions of *FLT1*, introns 4, 6, 9, and 10. Work with other disease-associated polymorphisms has demonstrated that noncoding SNPs may represent markers for tagged mutations or alter silencer or enhancer regions.[69,70] Sequencing of the flanking exons and exon/intron boundaries in the discovery family-based cohort did not identify any coding SNPs or other variants that were associated with AMD; therefore, it does not appear that any of the five significant SNPs tag for any functional mutations. Furthermore, it is unclear whether these SNPs contribute to the overall regulation of FLT1 expression. Serum analysis of individuals within this same cohort demonstrates no significant difference in sFLT1 levels in the serum of related individuals with or without AMD (Table 3). However, significant interaction seen was between sFLT1 and *FLT1* SNPs rs9943922 and rs7324510 (Table 3). Specifically, there was elevated sFLT1 in the serum of controls who had one or more copies of the risk allele, and most notably, those homozygous for the risk alleles of *FLT1* SNPs rs9943922 and rs7324510 (Fig. 1). One interpretation of this is that elevated sFLT1 protects those normal subjects from the AMD risk conferred by these risk alleles at SNPs rs9943922 and rs7324510. This is consistent with the known biologic function of sFLT1 as an angiogenic antagonist. The level and translated form of FLT1 within the retina is not known for patients with these significant *FLT1* SNPs. Further, the role of systemic sFLT1 in patients with neovascular AMD also is not known. Animal models of laser-induced CNV do demonstrate upregulation of VEGFR1 at the level of the CNV lesions, though to our knowledge there are no data regarding serum FLT1 analysis in animal models of neovascular AMD.[65] Analysis of the specific effect of these SNPs on systemic and retinal FLT1 expression, with regard to quantity and mature protein form, is an important future question.

In silico analysis is an important screening tool for prediction of functional consequence when changes are found at the DNA level. Our in silico analysis revealed potential splice site alterations within introns 10, 4, and 6. Specifically, the presence of the minor allele for SNP rs9508034 within intron 10 alters a constitutive acceptor site resulting in slightly decreased activity. This analysis also demonstrates formation of a novel acceptor site formation within intron 4 in the presence of rs9513115. Finally, presence of the minor allele for SNP rs7324510 is predicted to create a novel donor and acceptor splice site within intron 4. Our in silico analysis of RNA secondary structure demonstrated that each of the five significant *FLT1* SNPs alters potential folding. This may alter RNA function in a number of ways; one important consideration is the possible change in production of noncoding RNA (nc-RNA). Recent data suggest that noncoding SNPs can result in functional changes through changes in nc-RNA structures.[71] The decrease in energy required for folding in three of the five *FLT1* SNPs favors this hypothesis, as decreased folding energy, presence of specific RNA conformations, and evolutionary sequence conservation are critical factors for expression of known nc-RNA.[71] Though there are no known noncoding RNA structures within the introns containing the significant *FLT1* SNPs, the predicted secondary RNA conformations for minor allele sequences makes this an intriguing possibility. Further

Table 4. Summary of In Silico Proposed *FLT1* SNP Function

FLT1 SNP	In Silico Splice Site Analysis	In Silico Methylation Analysis	In Silico RNA Secondary Structure Analysis	Literature Review
rs9508034: Intron 10	Change to a constitutive acceptor site	No difference	Altered secondary structure, decreased energy of folding for the minor allele	1. Proposed regulatory function for HLA-Cw which has been associated with development of AMD 2. Associated with development of breast cancer
rs9513115: Intron 4	Analysis of potential alternative splice sites reveals a novel acceptor site formation	No difference	Altered secondary structure, decreased energy of folding for the minor allele	Associated with development of breast cancer
rs2281827: Intron 9	No Change	No difference	Altered secondary structure, decreased energy of folding for the minor allele	Significantly associated with retinal arteriolar caliber
rs9943922: Intron 10	No Change	No difference	Altered secondary structure, increased energy of folding for the minor allele	Associated with development of breast cancer
rs7324510: Intron 6	Formation of novel acceptor and donor splice sites	No difference	Altered secondary structure, increased energy of folding for the minor allele	Proposed regulatory function for cyclin B1 interacting protein 1

work, including RNA-seq analysis and functional assays, is needed to more fully characterize the implication of these polymorphisms on RNA structure, protein expression, and function.

Each of the five *FLT1* SNPs identified within our cohorts has been described previously in the literature, although to our knowledge this study is the first to show genetic association between *FLT1* SNPs and AMD. SNP rs2281827 has been found to be associated with retinal arteriolar caliber.[72] Hypertension and hyperlipidemia, both of which alter arteriolar caliber, are known risk factors for development of AMD.[1,73] Therefore, further work to understand the role of this *FLT1* SNP may increase our understanding of disease pathogenesis as it relates to established risk factors. In addition, three of the five *FLT1* polymorphisms we describe here, rs9513115, rs9943922, and rs9508034, have been associated with the development of breast cancer, a disease that has been treated clinically with anti-VEGF therapies as angiogenesis is fundamental to its pathogenesis.[74,75] Thus, the influence of these polymorphisms on FLT1 expression and/or function may not be confined to AMD pathogenesis.

Taken together, our data supported the idea that genetic variation in *VEGFA* and *KDR* is not associated significantly with the presence of neovascular AMD pathology. To substantiate this further, we assessed variants suggested to be associated with neovascular AMD in the literature. While initially significant in our study, polymorphisms in *KDR* (rs1531289) and *VEGFA* (rs833061), previously associated with AMD risk, did not remain significant after meta-analysis in our cohorts.[28,33] Furthermore, analysis of AMD-associated *VEGFA* SNPs rs13207351, rs1570360, rs2010963, rs1413711, rs833070, rs735286, rs3025020, rs3025021, rs3025039, and rs3025033,[32,40] and coronary heart disease–associated *KDR* SNP rs1870377[41] also showed no association in our cohorts. Interestingly, like in our study, Churchill et al.[27] found no association between single SNPs in the *VEGFA* 5′UTR/promoter and AMD. Conversely, they did find association between AMD and a 5-SNP haplotype, including tagging SNPs overlapping with those investigated in our study, spanning the entire *VEGFA* gene, while in our study we found no haplotype in *VEGFA* more significantly associated with AMD than any single SNP.

FLT1 May Be Regulated by Nr2e3 Within AMD

Data presented here further supported a role for FLT1 in AMD pathogenesis, and, thus, increases the possible significance of *FLT1* genetic variation. Though suggested in the literature, the mechanism for *FLT1* regulation in AMD is not clear. Our work has identified a response element site in the 5′ untranslated region of murine *FLT1* which binds Nr2e3. Prior work demonstrates that Nr2e3 may regulate genes involved in AMD pathogenesis. Therefore, *FLT1* is now placed in a nuclear hormone receptor–modulated AMD transcriptional network.[56] Further work, including RNA-seq analysis and functional assays, is needed to characterize more fully the implication of these polymorphisms on RNA structure and role of FLT1 in the overall pathogenesis of neovascular AMD.

Summary

The role of genetic variation in AMD risk is important with diagnostic, prognostic, and treatment implications, and current understanding of AMD risk due to genetic variation in VEGF pathway genes is incomplete. Although these SNPs do not have clear functional consequences, a number are suggested based on in silico analyses, known gene associations, and identification of these *FLT1* SNPs within the context of AMD and other disease pathogenesis (Table 4). The strongest data linking response to anti-VEGF treatment and VEGF pathway SNPs support our findings that these are significant disease-associated SNPs within *FLT1* and this may influence development of disease as well as treatment response. Finally, we also showed potential regulation of *FLT1* expression by Nr2e3 through binding of a regulatory domain. Taken together these data demonstrate that FLT1 may have an important role in AMD pathogenesis. Current therapies do not specifically account for the role of FLT1 in AMD. Further elucidation of the functional role for significant *FLT1* variants will aid in efficacious therapeutic FLT1 targeting. Importantly, *FLT1* variants identi-

fied in our work are significant across multiple ethnic backgrounds and, therefore, therapeutic strategies using these data may be applicable globally.

Acknowledgments

Supported by NIH Grant EY-014458, the ALSAM Foundation, the Edward N. & Della L. Thome Memorial Fund, the Lincy Foundation, Bausch & Lomb, National Research Foundation of Korea grants funded by the Ministry of Education, Science and Technology (2012R1A1A2008943), and an unrestricted grant from the Research to Prevent Blindness Foundation to the University of Utah Department of Ophthalmology and Visual Sciences.

Disclosure: **L.A. Owen**, None; **M.A. Morrison**, None; **J. Ahn**, None; **S.J. Woo**, None; **H. Sato**, None; **R. Robinson**, None; **D.J. Morgan**, None; **F. Zacharaki**, None; **M. Simeonova**, None; **H. Uehara**, None; **U. Chakravarthy**, None; **R.E. Hogg**, None; **B.K. Ambati**, None; **M. Kotoula**, None; **W. Baehr**, None; **N.B. Haider**, None; **G. Silvestri**, Allergan (C), Bayer (C); **J.W. Miller**, Alcon (C), KalVista Pharmaceuticals (C), Regeneron Pharmaceuticals, Inc. (C), ISIS Pharmaceuticals, Inc. (C), Imagen Biotech, Inc. (C), ONL Therapeutics, LLC (C), Maculogix, Inc. (C); **E.E. Tsironi**, None; **L.A. Farrer**, None; **I.K. Kim**, ArticDx (C); **K.H. Park**, None; **M.M. DeAngelis**, None

References

1. Klein R, Klein BE, Knudtson MD, Meuer SM, Swift M, Gangnon RE. Fifteen-year cumulative incidence of age-related macular degeneration: the Beaver Dam Eye Study. *Ophthalmology*. 2007;114:253–262.
2. Jager RD, Mieler WF, Miller JW. Age-related macular degeneration. *N Engl J Med*. 2008;358:2606–2617.
3. Ding X, Patel M, Chan CC Molecular pathology of age-related macular degeneration. *Prog Retin Eye Res*. 2009;28:1–18.
4. Rahimi N. VEGFR-1 and VEGFR-2: two non-identical twins with a unique physiognomy. *Front Biosci J Virtual Libr*. 2006; 11:818–829.
5. Ferrara N, Gerber HP, LeCouter J. The biology of VEGF and its receptors. *Nat Med*. 2003;9:669–676.
6. Lukason M, DuFresne E, Rubin H, et al. Inhibition of choroidal neovascularization in a nonhuman primate model by intravitreal administration of an AAV2 vector expressing a novel anti-VEGF molecule. *Mol Ther*. 2011;19:260–265.
7. Hiratsuka S, Minowa O, Kuno J, Noda T, Shibuya M. Flt-1 lacking the tyrosine kinase domain is sufficient for normal development and angiogenesis in mice. *Proc Natl Acad Sci U S A*. 1998;95:9349–9354.
8. Lai CM, Shen WY, Brankov M, et al. Long-term evaluation of AAV-mediated sFlt-1 gene therapy for ocular neovascularization in mice and monkeys. *Mol Ther*. 2005;12:659–668.
9. Kendall RL, Thomas KA. Inhibition of vascular endothelial cell growth factor activity by an endogenously encoded soluble receptor. *Proc Natl Acad Sci U S A*. 1993;90:10705–10709.
10. Tolentino MJ, McLeod DS, Taomoto M, Otsuji T, Adamis AP, Lutty GA. Pathologic features of vascular endothelial growth factor-induced retinopathy in the nonhuman primate. *Am J Ophthalmol*. 2002;133:373–385.
11. Onami H, Nagai N, Kaji H, et al. Transscleral sustained vasohibin-1 delivery by a novel device suppressed experimentally-induced choroidal neovascularization. *PloS One*. 2013;8: e58580.
12. Shimizu K, Watanabe K, Yamashita H, et al. Gene regulation of a novel angiogenesis inhibitor, vasohibin, in endothelial cells. *Biochem Biophys Res Commun*. 2005;327:700–706.
13. Kimura H, Miyashita H, Suzuki Y, et al. Distinctive localization and opposed roles of vasohibin-1 and vasohibin-2 in the regulation of angiogenesis. *Blood*. 2009;113:4810–4818.
14. Oshima Y, Oshima S, Nambu H, et al. Increased expression of VEGF in retinal pigmented epithelial cells is not sufficient to cause choroidal neovascularization. *J Cell Physiol*. 2004;201: 393–400.
15. Spilsbury K, Garrett KL, Shen WY, Constable IJ, Rakoczy PE. Overexpression of vascular endothelial growth factor (VEGF) in the retinal pigment epithelium leads to the development of choroidal neovascularization. *Am J Pathol*. 2000;157:135–144.
16. Owen LA, Uehara H, Cahoon J, Huang W, Simonis J, Ambati BK. Morpholino-mediated increase in soluble Flt-1 expression results in decreased ocular and tumor neovascularization. *PloS One*. 2012;7:e33576.
17. Yamashita H, Abe M, Watanabe K, et al. Vasohibin prevents arterial neointimal formation through angiogenesis inhibition. *Biochem Biophys Res Commun*. 2006;345:919–925.
18. Onami H, Nagai N, Machida S, et al. Reduction of laser-induced choroidal neovascularization by intravitreal vasohibin-1 in monkey eyes. *Retina*. 2012;32:1204–1213.
19. Francis PJ. The influence of genetics on response to treatment with ranibizumab (Lucentis) for age-related macular degeneration: the Lucentis Genotype Study (an American Ophthalmological Society thesis). *Trans Am Ophthalmol Soc*. 2011;109: 115–156.
20. Fung AT, Kumar N, Vance SK, et al. Pilot study to evaluate the role of high-dose ranibizumab 2.0 mg in the management of neovascular age-related macular degeneration in patients with persistent/recurrent macular fluid <30 days following treatment with intravitreal anti-VEGF therapy (the LAST Study). *Eye (Lond)*. 2012;26:1181–1187.
21. CATT Research Group, Martin DF, Maguire MG, et al. Ranibizumab and bevacizumab for neovascular age-related macular degeneration. *N Engl J Med*. 2011;364:1897–1908.
22. Lim LS, Mitchell P, Seddon JM, Holz FG, Wong TY. Age-related macular degeneration. *Lancet*. 2012;379:1728–1738.
23. Deangelis MM, Silveira AC, Carr EA, Kim IK. Genetics of age-related macular degeneration: current concepts, future directions. *Semin Ophthalmol*. 2011;26:77–93.
24. Fritsche LG, Chen W, Schu M, et al. Seven new loci associated with age-related macular degeneration. *Nat Genet*. 2013;45: 433–439, 439e1–e2.
25. Gorin MB. Genetic insights into age-related macular degeneration: controversies addressing risk, causality, and therapeutics. *Mol Aspects Med*. 2012;33:467–486.
26. Swaroop A, Chew EY, Rickman CB, Abecasis GR. Unraveling a multifactorial late-onset disease: from genetic susceptibility to disease mechanisms for age-related macular degeneration. *Annu Rev Genomics Hum Genet*. 2009;10:19–43.
27. Churchill AJ, Carter JG, Lovell HC, et al. VEGF polymorphisms are associated with neovascular age-related macular degeneration. *Hum Mol Genet*. 2006;2955–2961.
28. Szaflik JP, Blasiak J, Kryzanowska A, et al. Distribution of the C-460T polymorphism of the vascular endothelial growth factor gene in age-related macular degeneration. *Klin Oczna*. 2009; 111:125–127.
29. Yu Y, Bhangale TR, Fagerness J, et al. Common variants near FRK/COL10A1 and VEGFA are associated with advanced age-related macular degeneration. *Hum Mol Genet*. 2011;20: 3699–3709.
30. Huang C, Xu Y, Li X, Wang W. Vascular endothelial growth factor A polymorphisms and age-related macular degeneration: a systematic review and meta-analysis. *Mol Vis*. 2013;19:1211–1221.
31. SanGiovanni JP, Chen J, Sapieha A, et al. DNA sequence variants in PPARGC1A, a gene encoding a coactivator of the ω-3 LCPUFA sensing PPAR-RXR transcription complex, are associated with NV AMD and AMD-associated loci in genes

of complement and VEGF signaling pathways. *PloS One*. 2013; 8:e53155.

32. Haines JL, Schnetz-Boutad N, Schmidt S, et al. Functional candidate genes in age-related macular degeneration: significant association with VEGF, VLDLR, and LRP6. *Invest Ophthalmol Vis Sci*. 2006;47:329–335.
33. Sharma NK, Gupta A, Prabhakar S, Singh R, Sharma S, Anand A. Single nucleotide polymorphism and serum levels of VEGFR2 are associated with age related macular degeneration. *Curr Neurovasc Res*. 2012;9:256–265.
34. Chen W, Stambolian D, Edwards AO, et al. Genetic variants near TIMP3 and high-density lipoprotein-associated loci influence susceptibility to age-related macular degeneration. *Proc Natl Acad Sci U S A*. 2010;107:7401–7406.
35. Deangelis MM, Ji F, Adams S, et al. Alleles in the HtrA serine peptidase 1 gene alter the risk of neovascular age-related macular degeneration. *Ophthalmology*. 2008;115:1209–1215.e7,
36. DeAngelis MM, Lane AM, Shah CP, Ott, J, Dryla TP, Miller JW. Extremely discordant sib-pair study design to determine risk factors for neovascular age-related macular degeneration. *Arch Ophthalmol*. 2004;122:575–580.
37. Age-Related Eye Disease Study Research Group. A randomized, placebo-controlled, clinical trial of high-dose supplementation with vitamins C and E, beta carotene, and zinc for age-related macular degeneration and vision loss: AREDS report no. 8. *Arch Ophthalmol*. 2001;119:1417–1436.
38. McKay GJ, Dasari S, Patterson CC, Chakravarthy U, Silvestri G. Complement component 3: an assessment of association with AMD and analysis of gene-gene and gene-environment interactions in a Northern Irish cohort. *Mol Vis*. 2010;16: 194–199.
39. Silveira AC, Morrison MA, Ji, F, et al. Convergence of linkage, gene expression and association data demonstrates the influence of the RAR-related orphan receptor alpha (RORA) gene on neovascular AMD: a systems biology based approach. *Vision Res*. 2010;50:698–715.
40. Fang AM, Lee AY, Kulkarni M, Osborn MP, Brantley MA Jr. Polymorphisms in the VEGFA and VEGFR-2 genes and neovascular age-related macular degeneration. *Mol Vis*. 2009; 15:2710–2719.
41. Ellis SG, Chen MS, Jia G, Luke M, Cassano J, Lytle B. Relation of polymorphisms in five genes to long-term aortocoronary saphenous vein graft patency. *Am J Cardiol*. 2007;99:1087–1089.
42. Menendez D, Krysiak O, Inga A, Krysiak B, Resnick MA, Schönfelder G. A SNP in the flt-1 promoter integrates the VEGF system into the p53 transcriptional network. *Proc Natl Acad Sci U S A*. 2006;103:1406–1411.
43. Srivatsan A, Han Y, Peng J, et al. High-precision, whole-genome sequencing of laboratory strains facilitates genetic studies. *PLoS Genet*. 2008;4:e1000139.
44. Dudbridge F. Likelihood-based association analysis for nuclear families and unrelated subjects with missing genotype data. *Hum Hered*. 2008;66:87–98.
45. Han F, Pan W. A data-adaptive sum test for disease association with multiple common or rare variants. *Hum Hered*. 2010;70: 42–54.
46. Wang M, Marín A. Characterization and prediction of alternative splice sites. *Gene*. 2006;366:219–227.
47. Mollema NJ, Yuan Y, Jelcick AS, et al. Nuclear receptor Rev-erb alpha (Nr1d1) functions in concert with Nr2e3 to regulate transcriptional networks in the retina. *PloS One*. 2011;6: e17494.
48. Haider NB, Mollema N, Gaule M, et al. Nr2e3-directed transcriptional regulation of genes involved in photoreceptor development and cell-type specific phototransduction. *Exp Eye Res*. 2009;89:365–372.
49. Hu M, Shi H, Xu Z, Liu W. Association between epidermal growth factor gene rs4444903 polymorphism and risk of glioma. *Tumour Biol*. 2013;34:1879–1885.
50. Coiffier B, Li W, Henitz ED, et al. Prespecified candidate biomarkers identify follicular lymphoma patients who achieved longer progression-free survival with bortezomib-rituximab versus rituximab. *Clin Cancer Res*. 2013;19:2551–2561.
51. Firth M, Hamada M, Horton P. Parameters for accurate genome alignment. *BMC Bioinformatics*. 2010;11:80.
52. Cheng H, Khanna H, Oh EC, Hicks D, Mitton KP, Swaroop A. Photoreceptor-specific nuclear receptor NR2E3 functions as a transcriptional activator in rod photoreceptors. *Hum Mol Genet*. 2004;13:1563–1575.
53. Haider NB, Demarco P, Nystuen AM, et al. The transcription factor Nr2e3 functions in retinal progenitors to suppress cone cell generation. *Vis Neurosci*. 2006;23:917–929.
54. Mollema N, Haider NB. Focus on molecules: nuclear hormone receptor Nr2e3: impact on retinal development and disease. *Exp Eye Res*. 2010;91:116–117.
55. Peng GH, Ahmad O, Ahmad F, Liu J, Chen S. The photoreceptor-specific nuclear receptor Nr2e3 interacts with Crx and exerts opposing effects on the transcription of rod versus cone genes. *Hum Mol Genet*. 2005;14:747–764.
56. Jelcick AS, Yuan Y, Leehy BD, et al. Genetic variations strongly influence phenotypic outcome in the mouse retina. *PloS One*. 2011;6:e21858.
57. Velez-Montoya R, Oliver SC, Olson JL, et al. Current knowledge and trends in age-related macular degeneration: today's and Future Treatments. *Retina*. 2012;33:1487–1502.
58. Ferrara N, Davis-Smyth T. The biology of vascular endothelial growth factor. *Endocr Rev*. 1997;18:4–25.
59. Ferrara N. Role of vascular endothelial growth factor in regulation of physiological angiogenesis. *Am J Physiol Cell Physiol*. 2001;280:C1358–C1366.
60. Shibuya M. Vascular endothelial growth factor receptor-1 (VEGFR-1/Flt-1): a dual regulator for angiogenesis. *Angiogenesis*. 2006;9:225–230, discussion 231.
61. Veikkola T, Karkkainen M, Claesson-Welsh L, Alitalo K. Regulation of angiogenesis via vascular endothelial growth factor receptors. *Cancer Res*. 2000;.60:203–212.
62. Hiratsuka S, Maru Y, Okada A, Seiki M, Noda T, Shibuya M. Involvement of Flt-1 tyrosine kinase (vascular endothelial growth factor receptor-1) in pathological angiogenesis. *Cancer Res*. 2001;61:1207–1213.
63. Kim H, Choi JS, Kim KS, Yang JA, Hahn SK. Flt1 peptide-hyaluronate conjugate micelle-like nanoparticles encapsulating genistein for the treatment of ocular neovascularization. *Acta Biomater*. 2012;8:3932–3940.
64. Fischer C, Mazzone M, Jonckx B, Carmeliet P. FLT1 and its ligands VEGFB and PlGF: drug targets for anti-angiogenic therapy? *Nat Rev Cancer*. 2008;8:942–956.
65. Huang H, Shen J, Vinores SA. Blockade of VEGFR1 and 2 suppresses pathological angiogenesis and vascular leakage in the eye. *PloS One*. 2011;6:e21411.
66. Luttun A, Tjwa M, Moons L, et al. Revascularization of ischemic tissues by PlGF treatment, and inhibition of tumor angiogenesis, arthritis and atherosclerosis by anti-Flt1. *Nat Med*. 2002;8:831–840.
67. Carmeliet P, Moons L, Lutton A, et al. Synergism between vascular endothelial growth factor and placental growth factor contributes to angiogenesis and plasma extravasation in pathological conditions. *Nat Med*. 2001;7:575–583.

Investigative Ophthalmology & Visual Science

68. Van de Veire S, Stalmans I, Heindryckx F, et al. Further pharmacological and genetic evidence for the efficacy of PlGF inhibition in cancer and eye disease. *Cell*. 2010;141:178–190.
69. Palmer CN, Irvine AD, Terron-Kwiatkowski A, et al. Common loss-of-function variants of the epidermal barrier protein filaggrin are a major predisposing factor for atopic dermatitis. *Nat Genet*. 2006;38:441–446.
70. Hugot JP, Chamaillard M, Zouali H, et al. Association of NOD2 leucine-rich repeat variants with susceptibility to Crohn's disease. *Nature*. 2001;411:599–603.
71. Esteller M. Non-coding RNAs in human disease. *Nat Rev Genet*. 2011;12:861–874.
72. Ikram MK, Sim X, Jensen RA, et al. Four novel Loci (19q13, 6q24, 12q24, and 5q14) influence the microcirculation in vivo. *PLoS Genet*. 2010;6:e1001184.
73. Javitt NB, Javitt JC. The retinal oxysterol pathway: a unifying hypothesis for the cause of age-related macular degeneration. *Curr. Opin. Ophthalmol*. 2009;20:151–157.
74. Beeghly-Fadiel A, Shu XO, Lu W, et al. Genetic variation in VEGF family genes and breast cancer risk: a report from the Shanghai Breast Cancer Genetics Study. *Cancer Epidemiol. Biomarkers Prev*. 2011;20:33–41.
75. Nieto Y, Woods J, Nawaz F, et al. Prognostic analysis of tumour angiogenesis, determined by microvessel density and expression of vascular endothelial growth factor, in high-risk primary breast cancer patients treated with high-dose chemotherapy. *Br J Cancer*. 2007;97:391–397.

Investigative Ophthalmology & Visual Science